# *A case study of boundary layer ventilation by convection and coastal processes*

Article

Published Version

JOURNAL OF GEOPHYSICAL RESEARCH, VOL. 112, D17106, doi:10.1029/2006JD007984, 2007



# A case study of boundary layer ventilation by convection and coastal processes

H. F. Dacre,[1] S. L. Gray,[1] and S. E. Belcher[1]

Received 31 August 2006; revised 23 February 2007; accepted 4 June 2007; published 12 September 2007.

[1] It is often assumed that ventilation of the atmospheric boundary layer is weak in the absence of fronts, but is this always true? In this paper we investigate the processes responsible for ventilation of the atmospheric boundary layer during a nonfrontal day that occurred on 9 May 2005 using the UK Met Office Unified Model. Pollution sources are represented by the constant emission of a passive tracer everywhere over land. The ventilation processes observed include shallow convection, turbulent mixing followed by large-scale ascent, a sea breeze circulation and coastal outflow. Vertical distributions of tracer are validated qualitatively with AMPEP (Aircraft Measurement of chemical Processing Export fluxes of Pollutants over the UK) CO aircraft measurements and are shown to agree impressively well. Budget calculations of tracers are performed in order to determine the relative importance of these ventilation processes. Coastal outflow and the sea breeze circulation were found to ventilate 26% of the boundary layer tracer by sunset of which 2% was above 2 km. A combination of coastal outflow, the sea breeze circulation, turbulent mixing and large-scale ascent ventilated 46% of the boundary layer tracer, of which 10% was above 2 km. Finally, coastal outflow, the sea breeze circulation, turbulent mixing, large-scale ascent and shallow convection together ventilated 52% of the tracer into the free troposphere, of which 26% was above 2 km. Hence this study shows that significant ventilation of the boundary layer can occur in the absence of fronts (and thus during high-pressure events). Turbulent mixing and convection processes can double the amount of pollution ventilated from the boundary layer.

**Citation:** Dacre, H. F., S. L. Gray, and S. E. Belcher (2007), A case study of boundary layer ventilation by convection and coastal processes, *J. Geophys. Res.*, *112*, D17106, doi:10.1029/2006JD007984.

## 1. Introduction

[2] Much of the pollution in the atmosphere originates from emissions in the atmospheric boundary layer, the region of the atmosphere closest to the Earth's surface where the properties of air parcels are strongly modified by the presence of the Earth's surface. The depth of this layer is variable, changing with location, time of day and meteorological situation. A stable layer at the top of the boundary layer often separates boundary layer air from air that is not affected by the Earth's surface, known as the free troposphere. This stable layer can inhibit the transport of air from the boundary layer to the free troposphere. In the boundary layer we often observe lower wind speeds than in the free troposphere and a different wind direction due to surface friction. Thus if pollution remains trapped within the boundary layer it typically does not travel far and can build up to become a local air pollution problem. In the free troposphere there is no dry deposition to the surface and most rates of chemical transformation are lower because of colder temperatures. Colder temperatures can enhance solubility and hence wet deposition of pollutants [*Hobbs*, 2000] but typically pollutants in the free troposphere have longer lifetimes than in the boundary layer. Thus if pollutants are transported to the free troposphere from the boundary layer, the longer lifetimes and higher wind speeds may greatly expand their range of influence and the local air pollution problem can become a regional or even a global problem. Therefore boundary layer ventilation is a key process in linking local air quality and global climate change.

[3] To explain the distribution of chemical species in the free troposphere it is important to understand both the chemistry and the dynamical processes responsible for the transport of pollution. Observational and modeling studies have shown that a wide range of processes may be important for boundary layer ventilation.

[4] 1. Advective processes include transport by the warm and cold conveyor belts associated with frontal systems [*Kowol-Santen et al.*, 2001; *Donnell et al.*, 2001; *Esler et al.*, 2003; *Agustí-Panareda et al.*, 2005], sea breeze circulations and coastal outflow [*Lu and Turco*, 1994; *Leon et al.*, 2001; *Angevine et al.*, 2006; *Verma et al.*, 2006] and mountain venting [*Lu and Turco*, 1994; *Baltensperger et al.*, 1997; *Seibert et al.*, 1998; *Kossmann et al.*, 1999].

[1]Department of Meteorology, University of Reading, Reading, UK.


0148-0227/07/2006JD007984$09.00

[5] 2. Mixing processes include deep convection [*Dickerson et al.*, 1987; *Lu and Turco*, 1994; *Hauf et al.*, 1995; *Wang and Prinn*, 2000], shallow convection [*Flatøy and Hov*, 1995; *Edy et al.*, 1996; *Gimson*, 1997], frontal convection [*Esler et al.*, 2003; *Agustí-Panareda et al.*, 2005], and boundary layer turbulence [*Angevine et al.*, 2006; *Verma et al.*, 2006].

[6] The relative importance of these transport mechanisms is not well known and is likely to depend on the synoptic situation under consideration.

[7] It is often assumed that there is little ventilation of the atmospheric boundary layer into the free troposphere during nonfrontal days, so that pollutant levels simply build up in the boundary layer. This is probably a good assumption on days on which there is no observed convection. Nevertheless, shallow convection is a common feature during nonfrontal days over Europe in the summer.

[8] In this paper we concentrate on the transport processes that occur during a nonfrontal day. A high-pressure region was situated to the west of the UK on this day. The event was simulated using the UK Met Office nonhydrostatic Unified Model. This case study was chosen because we are interested in ventilation of pollution in the absence of fronts and on days characterized by widespread shallow convection. This will provide insight into ventilation mechanisms that can occur on high-pressure days. Also, this case occurred during the Aircraft Measurement of chemical Processing Export fluxes of Pollutants over the UK (AMPEP) field campaign on which measurements of pollution were carried out (http://badc.nerc.ac.uk/data/polluted-tropo/projects/ampep.html). This allows us to qualitatively compare results from the model with observations. We aim to address two questions. First, can a mesoscale model simulate pollution transport in a manner consistent with the observations? This question needs to be addressed to determine which ventilation processes are realistically represented by the model. Second, by what ventilation processes does polluted boundary layer air enter the free troposphere in the absence of fronts, and what are their relative importance?

[9] Nonfrontal processes for boundary layer ventilation are described in section 2. The model used in this paper is described briefly in section 3. In section 4 an overview of the case study is given. The numerical experiments have been performed using the UK Met Office Unified Model with passive tracers. The experimental details are described in section 5. The results from numerical experiments for the case study are described in section 6 and they are compared with observations from the AMPEP field campaign in section 7. Tracer budgets are calculated in section 8. Finally, in section 9 the main conclusions are given.

## 2. Processes for Boundary Layer Ventilation During Nonfrontal Days

[10] Here we briefly review previous research which has considered boundary layer ventilation by convection and sea breezes. These are the processes that could lead to transport during nonfrontal days. Ventilation by warm and cold conveyor belts is associated with frontal events and mountain venting is not significant over the UK. Hence these mechanisms are not discussed further here.

[11] *Chatfield and Crutzen* [1984] hypothesized that convective transport is a major redistributor of pollutants from the boundary layer to the free atmosphere. Rapid updraughts are effective in ventilating the boundary layer and raising pollutants through many kilometers in tens of minutes. Evaporatively cooled downdraughts can be effective in bringing pollution from the free atmosphere into the boundary layer. Boundary layer turbulence may then be an important process in bringing the pollutants down to the ground. There have been several studies investigating transport of pollution by deep (>10 km) convective thunderstorms, *Dickerson et al.* [1987], *Hauf et al.* [1995], *Wang and Prinn* [2000] and *Lu et al.* [2000]. Nevertheless, over the UK, such deep convection is rare compared to shallow (<5 km) convection. Daytime shallow cumulus clouds are common over the UK during the summer and so, even though shallow convection induces weaker vertical transport than deep convection, they can contribute to nonnegligible amounts of pollution transport. *Thompson et al.* [1994] constructed a regional budget for boundary layer CO over the central US for June. They calculated horizontal fluxes into and out of the boundary layer, surface fluxes due to anthropogenic emissions, biogenic sources and deposition, photochemical production and loss of CO, and vertical fluxes due to deep convection. They assumed that the budget residual was due to ventilation of the boundary layer by shallow cumulus clouds and synoptic-scale frontal weather systems. This residual was estimated to be about the same magnitude as the net CO flux due to deep convection. Although they did not calculate the CO fluxes due to shallow convection and synoptic-scale weather systems explicitly, their study suggests the importance of these processes.

[12] There have been a few studies carried out to investigate the transport of pollution by shallow convection. *Flatøy and Hov* [1995] in their 3-D Mesoscale Chemistry Transport model found that during a 10-day period, characterized by high pressure and frequent occurrences of cumulus convection over Europe, that convection dominates over the synoptic-scale vertical advection as a ventilation mechanism. Their continental study has a horizontal resolution of 150 km and coarse vertical resolution in the lower troposphere so it may not represent the ventilation of the boundary layer by convective and boundary layer turbulent mixing processes well. *Edy et al.* [1996] modeled CO redistribution by shallow convection over the Amazonian rain forest using a 2-D convective cloud model coupled with a chemical model. They showed that 40% of the pollution emitted below 500 m reached 2000 m in altitude. However, this simulation modeled the evolution of a single convective cloud over a period of 2 hours. It is not clear whether these results can be scaled up to represent the ventilation of the boundary layer by widespread shallow convection over an entire day. *Gimson* [1997] modeled pollution transport by shallow convective clouds in the air behind a cold front using the UK Met Office Unified Model. Tracer was emitted 500 m above the surface and was transported to upper levels by shallow convection with a local maxima found at cloud top level (4–5 km). Comparisons with large eddy model simulations were made but no comparison with observations were carried out.

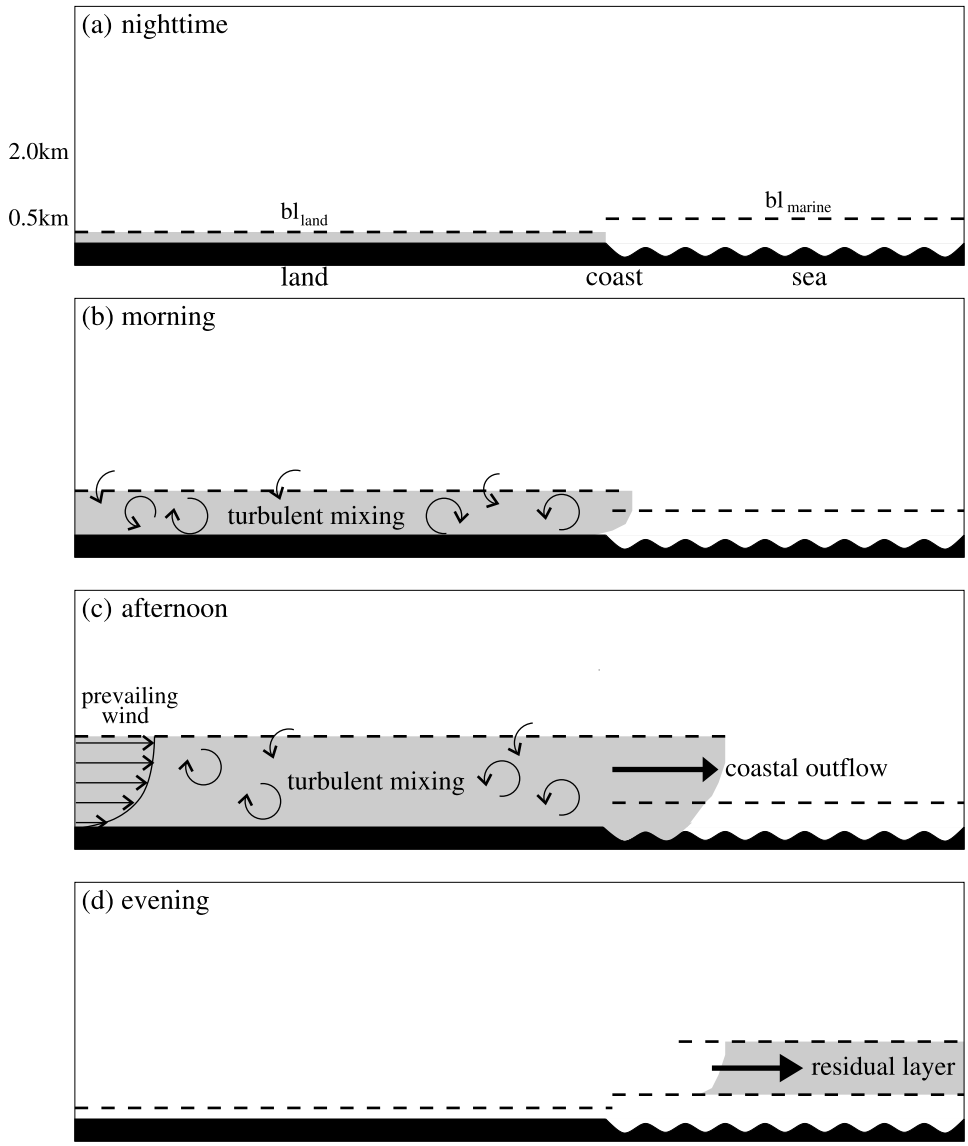


**Figure 1.** Schematic of coastal outflow. $bl_{land}$ and $bl_{marine}$ are stable layers at the top of the land and marine boundary layer respectively. Shading represents polluted air. (a) Pollution is emitted within the shallow boundary layer over land. (b) During the morning the boundary layer over land deepens, because of entrainment of free tropospheric air, and pollution is mixed throughout the depth of the boundary layer by turbulent mixing. (c) Pollution is advected over the sea by the prevailing wind. (d) Pollution above the marine boundary layer is trapped between two stable layers and becomes decoupled from the surface. This polluted layer can be transported long distances as there is no dry deposition to the surface.

[13] Several observational studies measuring aerosol in the atmosphere have found multiple aerosol layers located above the marine boundary layer [*Smith*, 1975; *Wakimoto and McElroy*, 1986; *Leon et al.*, 2001; *Angevine et al.*, 2006; *Verma et al.*, 2006]. It is hypothesized that the existence of these elevated layers is influenced by the diurnal variation in the structure of the upwind continental boundary layer. During the morning rapid growth of the continental boundary layer can mix pollutants through depths of 1000–2000 m. Over the ocean the sea surface temperature hardly changes between day and night, thus there is a much smaller diurnal cycle of the marine boundary layer resulting in nearly constant boundary layer depths typically about 500 m. This results in a decrease in boundary layer height at the coast. Pollution can be mixed up to the top of the boundary layer over land and then

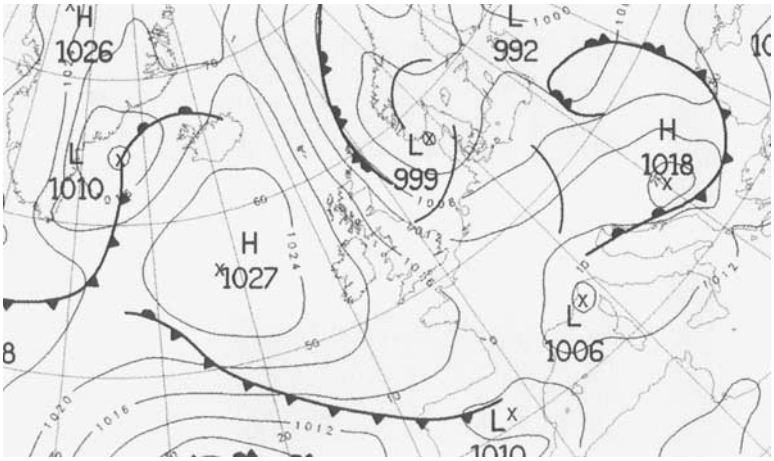


**Figure 2.** UK Met Office surface pressure analysis at 0000 UTC on 9 May 2005.

advected horizontally above the marine boundary layer. We term this process ''coastal outflow'' here (defined at the end of this section). Differential heating between the land and the sea also leads to the formation of a sea breeze. Collision between a sea breeze and the prevailing wind can result in polluted air being transported away from the Earth's surface. Further advection of this pollution across the coastline results in its ventilation from the boundary layer.

[14] A few studies have investigated the ventilation of pollution along the coast. *Schultz and Warner* [1982] carried out two-dimensional idealized simulations of pollution ventilation in the Los Angeles Basin. They found that for calm synoptic-scale wind conditions, sea breeze and mountain circulations dominated the ventilation. Ventilation was greatest in the vicinity of the sea breeze front. *Leon et al.* [2001] observed a layer of aerosol above the North Indian Ocean marine boundary layer. Their mesoscale modeling study showed that convergence between the sea breeze and the northeast monsoon winds along the west coast of India can transport air up to 2.5 km in altitude over land. However, the katabatic winds associated with the steep orography in this region may enhance the sea breeze circulation making it difficult to isolate the sea breeze as a ventilation process. *Lu and Turco* [1994] carried out idealized 2-D modeling of sea breeze and mountain ventilation and found that sea breezes as well as upslope winds both create vertical transport that can lead to the formation of elevated pollution layers. When mountains are close to the coastline, the sea breeze and mountain flows are strongly coupled.

[15] In this paper the term coastal outflow is used to describe the decoupling of pollution from the surface via the formation of an internal stable boundary layer which occurs when there is horizontal transport from land to sea and the

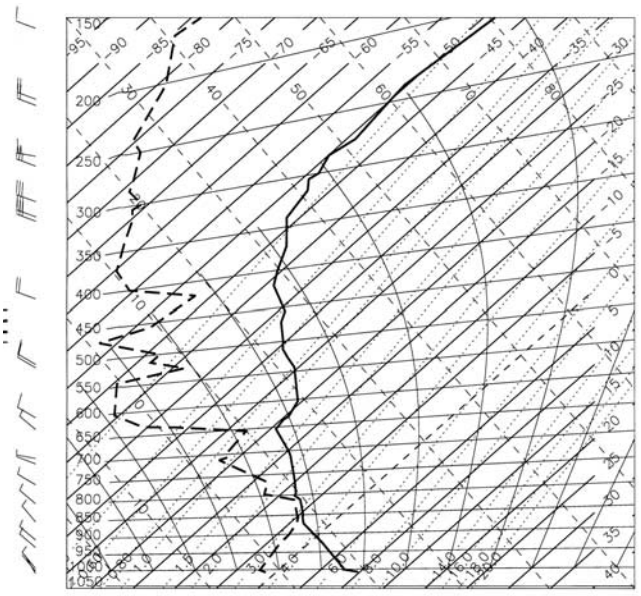

**Figure 3.** Tephigram from 1200 UTC 9 May 2005 Waddington RAF (53°N, 0°W, shown on Figure 5a).

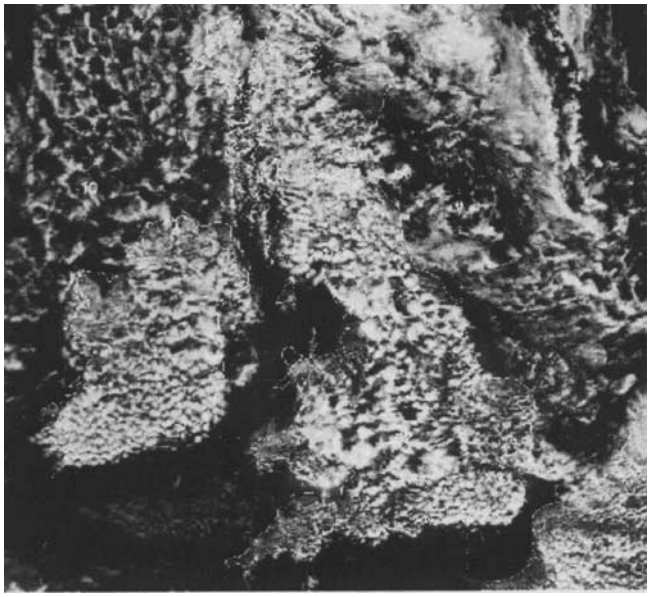

**Figure 4.** Visible image of the UK from the Modis Aqua satellite at 1245 UTC on 9 May 2005. Courtesy of NASA Goddard Space Flight Center.

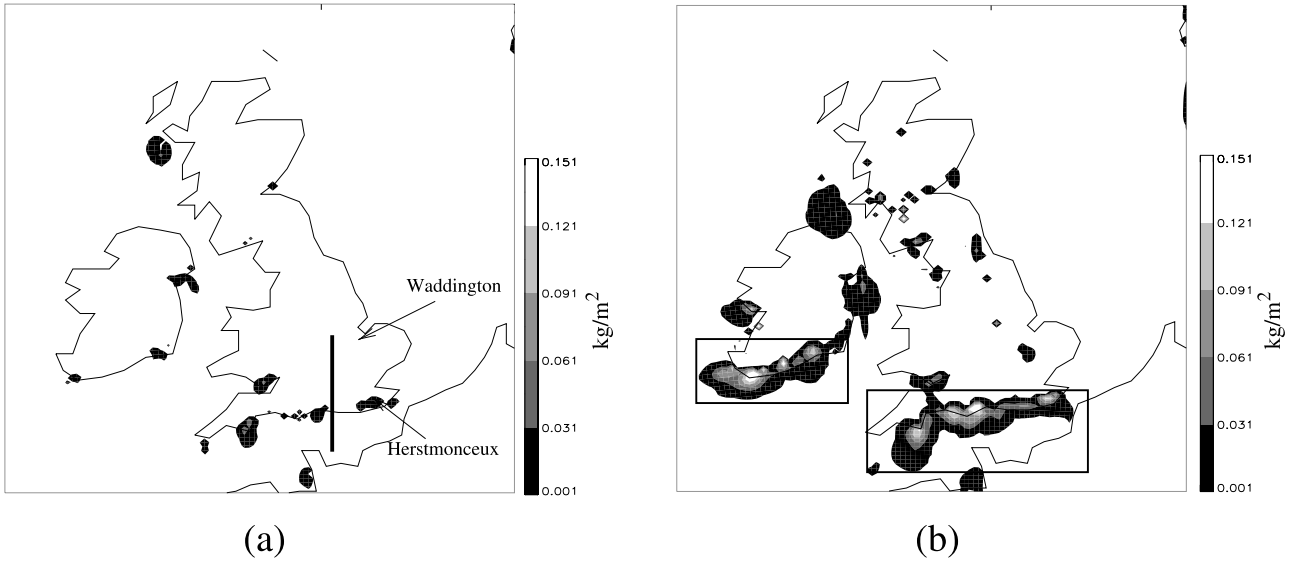


**Figure 5.** Tracer in the free troposphere integrated over height, contours every 0.03 kg/m$^2$ at (a) 1300 UTC and (b) 1700 UTC. Tracer is transported by advection only. Solid line indicates vertical cross section shown in Figures 6, 10, 13 and 15. Boxes indicate domain used in Figure 20c.

land boundary layer is deeper than the marine boundary layer (as is typically the case on summer days, see Figure 1). Ventilation is used loosely to encompass any process leading to the decoupling of pollutants from the surface. Thus we include coastal outflow in this definition although it is not strictly a venting process.

[16] We have chosen a case study in which widespread shallow convection occurs over the UK. We aim to simulate the ventilation of pollution by shallow convection, the sea breeze circulation and coastal outflow and compare our model results with AMPEP aircraft observations.

## 3. UK Met Office Unified Model

[17] The case has been simulated using the UK Met Office Unified Model version 5.5. This is an operational forecast model that contains leading edge physics and dynamics. The model is a nonhydrostatic primitive equation model using a semi-implicit, semi-Lagrangian numerical scheme [*Cullen*, 1993]. The model includes a comprehensive set of parameterizations, including boundary layer [*Lock et al.*, 2000], mixed phase cloud microphysics [*Wilson and Ballard*, 1999] and convection [*Gregory and Rowntree*, 1990]. There is no explicit diffusion in the model. A limited area domain with horizontal resolution 0.11° (approx 12.5 km) was used over Europe extending from 44°N to 64°N latitude and 12°W to 16°E longitude. The model has 38 levels in the vertical on a stretched grid ranging from the surface to 5 hPa. This corresponds to approximately 100 m layer spacing in the boundary layer and 500 m layer spacing in the midtroposphere. The first tracer model level is at 20 m.

[18] The boundary layer in the model is defined by the number of turbulent mixing levels (NTML). For stable conditions this is the region in contact with the surface where the bulk Richardson number is smaller than 1. For unstable conditions an adiabatic moist parcel ascent is performed in the model; ascent is stopped when the parcel becomes negatively buoyant. If the layer is well mixed the NTML is set to the parcel ascent top (inversion height). If the layer is cumulus capped the NTML is set to the lifting condensation level (cloud base). Thus the NTML is a good representation of the boundary layer, defined as the layer where mixing down to the surface is possible over short timescales.

## 4. Overview of the Case Study

[19] Figure 2 shows the UK Met Office surface pressure analysis for 0000 UTC on 9 May 2005. A high-pressure region approached the UK from the west becoming centered over the UK at 2100 UTC on 10 May. Figure 3 shows a tephigram for 1200 UTC on 9 May 2005 launched at Waddington (53°N, 0°W). There are weak northerly winds near the surface and stronger northwesterly winds above 2 km. There is also evidence of layers of increased static stability at 1000 m and at 3500 m. Figure 4 shows a visible image from the Modis Aqua satellite at 1245 UTC on 9 May 2005. Surface heating led to the outbreak of widespread shallow convection over the whole of the UK on this day.

## 5. Tracer Experiments

[20] Tracer sources are represented in the model by a constant emission of tracer everywhere over land at a rate of $5 \times 10^{-7}$ kgm$^{-2}$s$^{-1}$ emitted 20 m above the surface. (Tracers are also initialized everywhere within the boundary layer (uniform concentration $1 \times 10^{-7}$ kg/kg for all tracers). However the source emissions rapidly swamp the initial conditions.) Although the numerical experiments are aimed at identifying processes, the value of emission rate is chosen to mimic CO emissions. Uniform emissions were used to enable the relative importance of the different mechanisms to be determined. Realistic emissions would enable quantitative comparison with observations. However, the interpre-

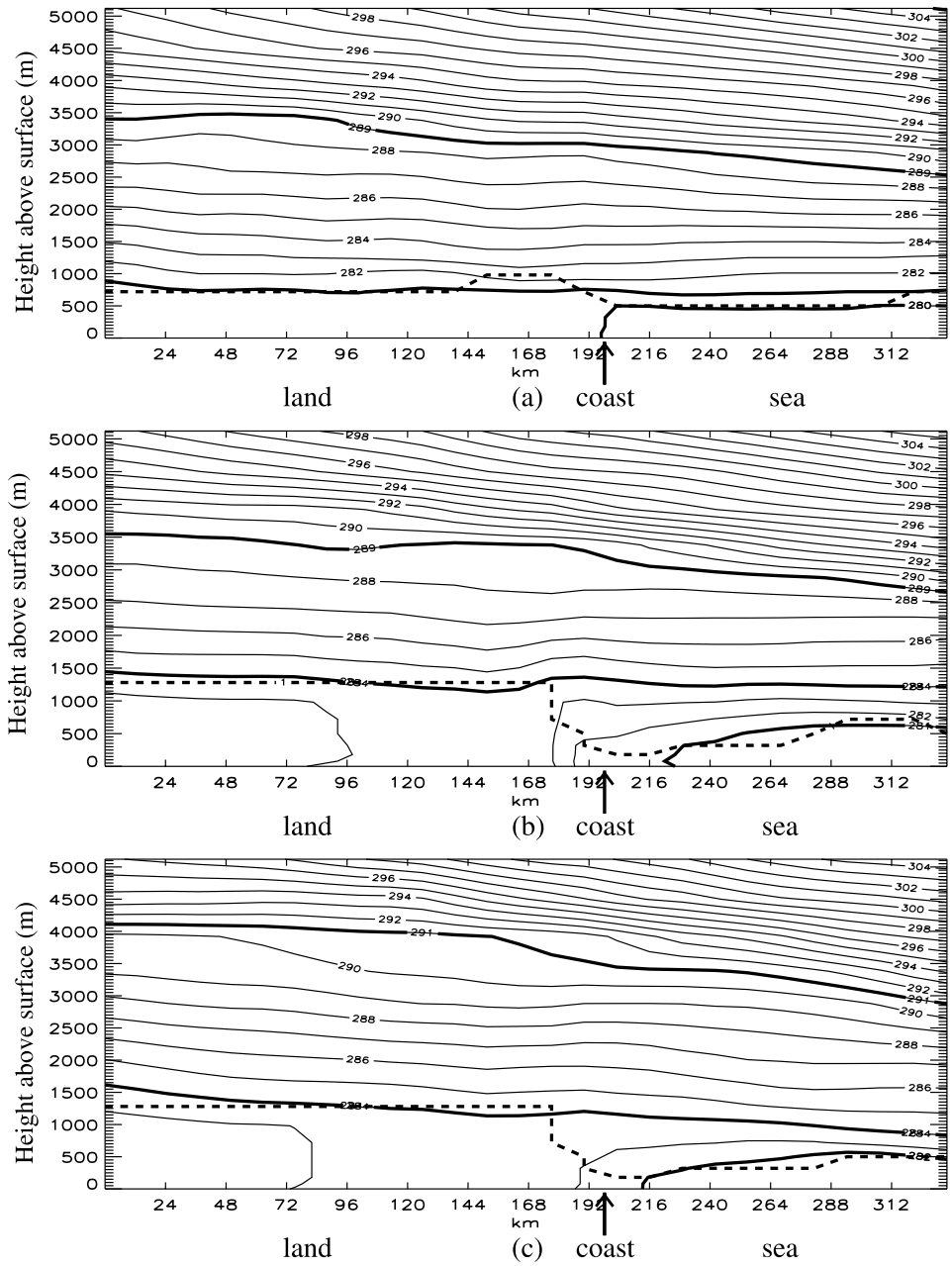


**Figure 6.** Vertical cross sections of potential temperature (solid). Bold contours indicate the $\theta$ contours that follow levels of increased static stability (not shown) overlaid with NTML (dashed) at (a) 0900 UTC, (b) 1300 UTC and (c) 1700 UTC.

tation of the results would be significantly complicated if the colocation of strong emission sources and localized ventilation mechanisms (such as convection and the sea breeze circulation) had to be considered.

[21] Four separate tracers have been used which are transported by different combinations of transport schemes, namely, the advection, convection and turbulent mixing schemes. The tracers in our simulation are treated as passive substances, meaning that they are subject to advection, convection and turbulent mixing but are neither deposited nor chemically transforming. This methodology, in which separate tracers transported by the schemes are used to attribute transport to different mechanisms, has also been used by *Donnell et al.* [2001], *Gray* [2003] and *Agustí-Panareda et al.* [2005].

## 6. Model Results

[22] First, the transport of the tracer which is advected only is described, second, the tracer that undergoes advection and turbulent mixing is described and finally, the tracer that undergoes advection, turbulent mixing and convection is described.

### 6.1. Advection Only

[23] Figure 5 shows the tracer in the free troposphere integrated over height for the case in which the tracer is

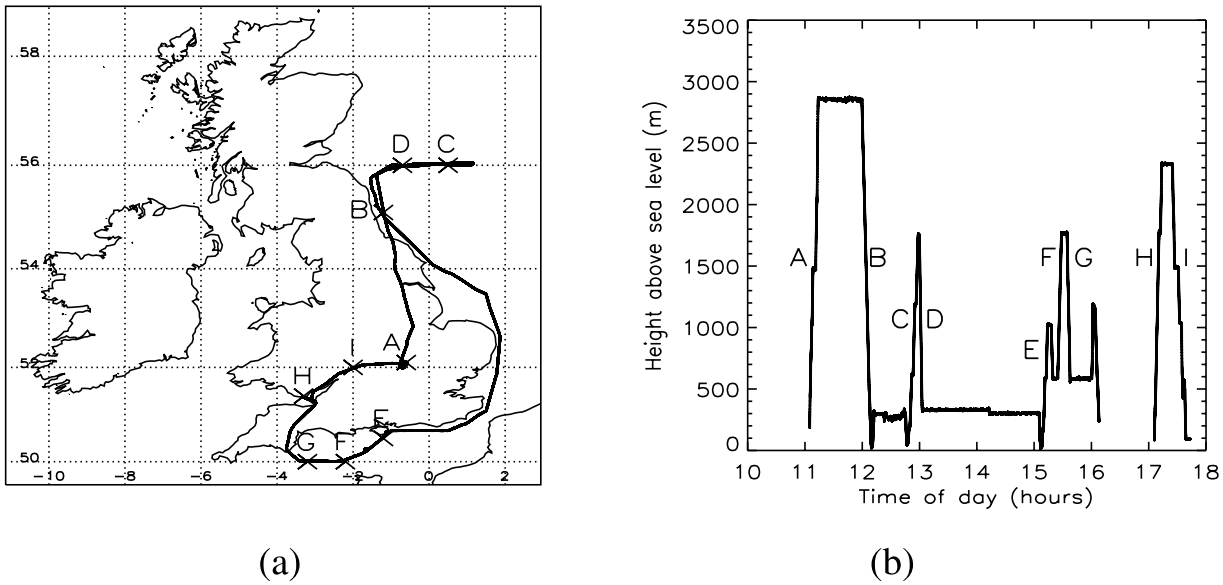


**Figure 7.** The 9 May 2005 AMPEP (a) flight path and (b) flight height. Profiles labeled A–I.

transported by advection only. The free troposphere is defined as being above the top of the boundary layer (defined by NTML, see section 3). There is no free tropospheric tracer at the start of the forecast as tracer is emitted 20 m above the surface. By 1300 UTC, Figure 5a, there is still very little tracer in the free troposphere. However, by 1700 UTC, Figure 5b, tracer is found in the free troposphere mainly located along the south coasts of England, Ireland and Wales.

[24] To determine the advective mechanism responsible for this boundary layer ventilation, vertical cross sections were taken along the line shown in Figure 5a. Vertical cross sections of potential temperature, $\theta$, are shown in Figure 6. Contours of $\theta$ that approximately follow layers of increased static stability (not shown) have been plotted in bold. At 0900 UTC, Figure 6a, a well mixed layer extends from the surface to 750 m over land and from the surface to 500 m over the sea. A weak stable layer separates the well mixed boundary layer air from free tropospheric air above. The stable layer over land is indicated by the bold $\theta$ = 281 K contour, and over the sea by the bold $\theta$ = 280 K contour. In the free atmosphere there is a strong stable layer indicated by the bold $\theta$ = 289 K contour which slopes from 3500 m over land to 2750 m over the sea. By 1300 UTC, Figure 6b, turbulent mixing over land has led to an increase in the height of the boundary layer up to 1300 m. The stable layers over land at the top of the boundary layer (1300 m) and in the free troposphere (3500 m) are consistent with the analyzed stable layers observed in the tephigram in Figure 3. Over the sea the well-mixed boundary layer depth has increased to 750 m. It can also be seen in Figure 6b that the land-sea temperature gradient, that was located at the coast in Figure 6a, has increased and penetrated further inland. This temperature gradient is known as the sea breeze front and it has been advected inland by a sea breeze. The sea breeze has a horizontal dimension of approximately 100 km and a vertical dimension of 300–400 m. Evidence of a sea breeze on this day is found in the surface observations. Herstmonceux (50.9°N, 0.3°E, shown on Figure 5a) shows a change in wind direction from 10° to 200°, a drop in temperature from 13° to 10° and an increase

**Table 1.** Summary of AMPEP Flight Profiles

| Profile | Summary |
|---|---|
| A | take off from Cranfield airport |
| B | NE coast: descent |
| C | clean air profile in North Sea: ascent |
| D | clean air profile in North Sea: descent |
| E | polluted profile in English Channel: ascent |
| F | polluted profile in English Channel: ascent |
| G | polluted profile in English Channel: descent |
| H | refuel and take off from Cardiff airport |
| I | land at Cranfield airport |

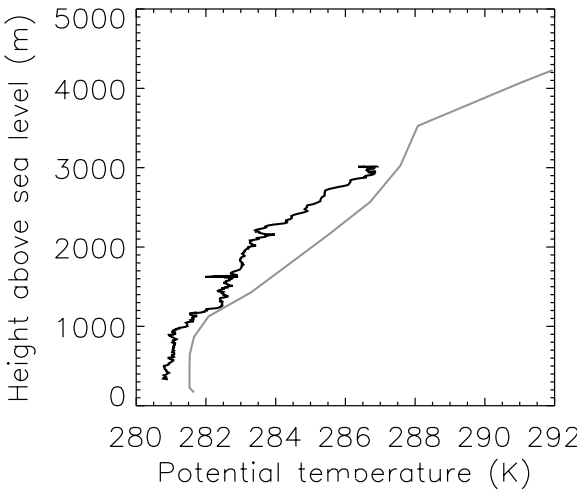


**Figure 8.** Model potential temperature profile A at 1100 UTC (grey) and AMPEP potential temperature profile A at 1105 UTC (black). Profile A location is shown in Figure 7a.

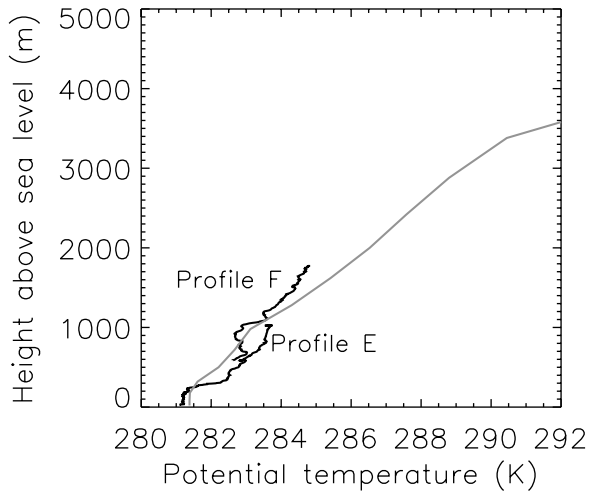


**Figure 9.** Model potential temperature profile E at 1500 UTC (grey) and AMPEP potential temperature profile E at 1506 UTC (black, 0–1000 m) and profile F at 1524 UTC (black, 600–1800 m). Profile E and F locations are shown in Figure 7a.

in humidity from 45% to 71% between 1200 UTC and 1300 UTC (not shown). By 1700 UTC, Figure 6c, the boundary layer heights are similar to those at 1300 UTC with the free atmospheric stable layer rising to 4000 m over land. The sea breeze front has retreated back toward the coastline. In Figures 6a–6c the dotted line represents the NTML. The NTML approximately follows the height of the lowest stable layer. This leads to a sharp decrease in boundary layer height on crossing from land to sea in the afternoon. Polluted air may be transported into the free troposphere here because of coastal outflow.

[25] On 9 May 2005 AMPEP performed a flight clockwise around England (Figure 7a). During the flight vertical profiles through the depth of the boundary layer were made. These profiles have been labeled A–I, Figure 7b, and are summarized in Table 1. Figure 8 shows the model $\theta$ profile at 1100 UTC and the AMPEP $\theta$ vertical profile at 1105 UTC taken in the middle of the UK (AMPEP profile A, location shown in Figure 7a). The model vertical profile shows a well mixed boundary layer extending from the surface to 1000 m. A stable layer at 1000 m separates the boundary layer air from the free tropospheric air. There is also a free tropospheric stable layer at 3500 m. The AMPEP $\theta$ vertical profile also shows a well mixed boundary layer with a depth of 1000 m. The free tropospheric stable layer is not captured as the profile only extends to 3000 m. Thus the model $\theta$ profile is consistent with the observations over land during the morning. Figure 9 shows the model $\theta$ profile at 1500 UTC and two AMPEP $\theta$ vertical profiles at 1506 UTC and 1524 UTC. These profiles are taken over the English Channel (AMPEP profiles E and F, locations shown in Figure 7a). The model profile shows two low-level stable layers, one at 300 m and another at 1000 m. There is also a free tropospheric stable layer at 3500 m. The AMPEP $\theta$ vertical profiles show stable layers at 300 m and 1000 m which are consistent with the model profiles. Thus we can conclude that the model representation of the stable layers shown in Figure 6 are also realistic over the sea.

[26] Figure 10 shows vertical cross sections of tracer concentration along the line shown in Figure 5a overplotted with the bold potential contours from Figures 6a–6c. Tracer is transported by advection only. Initially tracer remains near the surface in the lowest two model levels (Figure 10a). However at 1300 UTC, Figure 10b, tracer is advected up to 1000 m in height just inland from the coast. By 1700 UTC, Figure 10c, this tracer has been advected above the unpolluted marine boundary layer and mainly remains trapped between the two stable layers over the sea resulting in a layer of tracer above a layer with no tracer. The vertical transport of tracer away from the surface to the top of the boundary layer is due to convergence between the sea breeze and the prevailing northerly wind. Figure 11 shows the model vertical velocity at 1400 UTC, 500 m above the surface. The convergence line lies along the south coasts of England and Ireland. Tracer is advected vertically away from the surface to the top of the boundary layer. The tracer is then advected horizontally across the coast by the prevailing wind. Thus tracer is transported into the free troposphere above the marine boundary layer by the coastal outflow mechanism. Although there is a sea breeze acting in this case, a sea breeze is not needed for coastal outflow to occur. Turbulent mixing (seen in section 6.2) can also transport tracer up to the top of the boundary layer over land where it is then advected horizontally out of the boundary layer across the coast. A sea breeze can however increase the amount of pollution ventilated by coastal outflow. Advection across the coast could in part also be due to the return flow of the sea breeze circulation. Stronger offshore winds will lead to greater ventilation by coastal outflow but will prevent the sea breeze from penetrating onshore. Weaker offshore winds will reduce ventilation by coastal outflow but will allow the sea breeze to penetrate onshore resulting in greater ventilation by the sea breeze circulation.

[27] The advective mechanisms responsible for ventilating the boundary layer in this nonfrontal case are vertical advection, due to convergence between the sea breeze and the prevailing wind, and coastal outflow. Mountain venting and warm and cold conveyor belt advective transport are not observed. The overall importance of the sea breeze circulation and coastal outflow in ventilating the boundary layer is discussed in section 8.

### 6.2. Advection and Turbulent Mixing

[28] Figure 12 shows the tracer in the free troposphere integrated over height for the tracer transported by advection and boundary layer turbulent mixing. Turbulent mixing entrains tracer free air from above the boundary layer diluting the concentration of the tracer in the boundary layer. Thus the tracer concentrations are much reduced compared to the tracer transported by advection only. At 1300 UTC, Figure 12a, tracer has been transported out of the boundary layer along the south coasts of England, Ireland and Wales. Thus coastal outflow is observed earlier than when tracer is transported by advection only. There is also some free tropospheric tracer over land. By 1700 UTC, Figure 12b, tracer has been transported out of the boundary layer over much of the UK and Ireland. Figure 13 shows vertical cross sections of tracer concentration for the tracer transported by advection and turbulent mixing. At

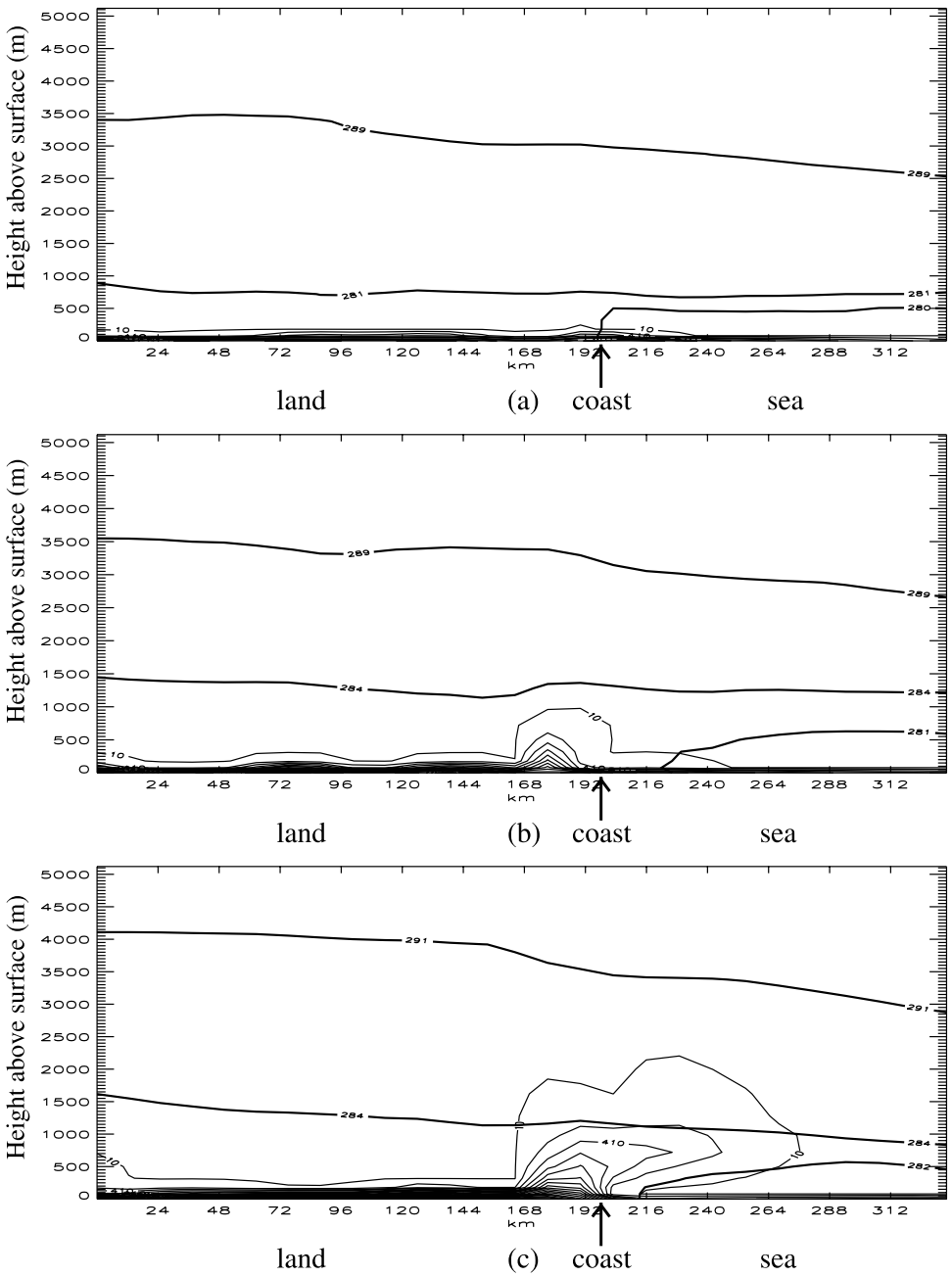


**Figure 10.** Vertical cross sections of tracer concentration, contours every $200 \times 10^{-7}$ kg/kg starting at $10 \times 10^{-7}$ kg/kg, overlaid with potential temperature contours from Figure 6, at (a) 0900 UTC, (b) 1300 UTC and (c) 1700 UTC. Tracer transported by advection only.

0900 UTC, Figure 13a, tracer has been mixed throughout the depth of the boundary layer over land. Tracer is advected off the coast over the sea, remaining within the marine boundary layer as in the advection only case.

[29] At 0900 UTC convergence over the sea allows a build up of tracer, emitted over land, to form off the south coast. By 1300 UTC, Figure 13b, the maximum in tracer concentration is now inland as for the advection only tracer, Figure 10b. Vertical motion, due to convergence between the sea breeze and the prevailing wind, transports some tracer out of the boundary layer at the coast. By 1700 UTC, Figure 13c, coastal outflow has advected high concentra-

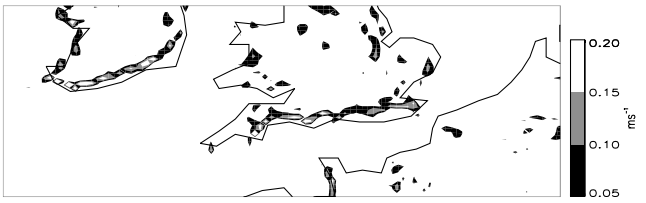


**Figure 11.** The 500 m vertical velocity at 1400 UTC, contours every 0.05 $ms^{-1}$.

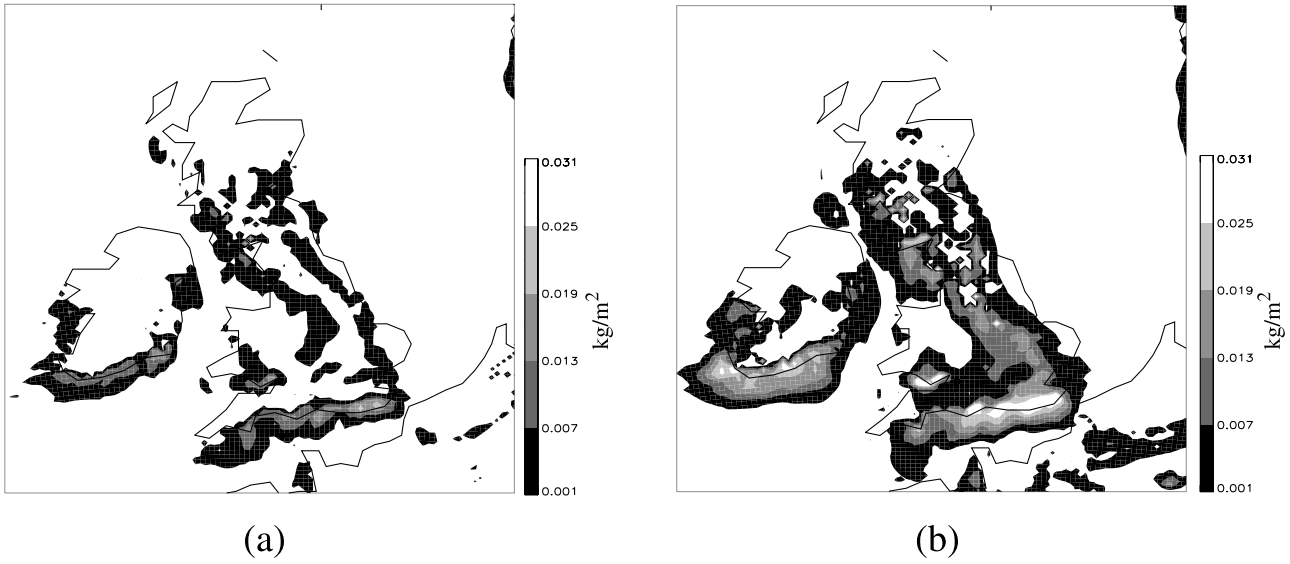


**Figure 12.** Tracer in the free troposphere integrated over height, contours every 0.006 kg/m$^2$ at (a) 1300 UTC and (b) 1700 UTC. Tracer transported by advection and turbulent mixing. Note the different shading scale to Figure 5.

tions of tracer above the marine boundary layer. Weak vertical ascent over the whole of the UK between 500 m and 4 km (not shown) advects tracer that has been mixed by turbulence within the boundary layer out of the boundary layer up to 2500 m. However, this tracer has not become separated from the boundary layer tracer and is transported at the same speed and in the same direction as the boundary layer tracer. The ascent rates at the boundary layer top are consistent with the distance traveled by the tracer. This implies that other processes that could lead to this transport, such as mixing in the stable air and numerical diffusion, are negligible.

[30] In summary, turbulent mixing is responsible for transporting tracer away from the surface and distributing it throughout the boundary layer. Turbulent mixing can also transport tracer to above the boundary layer top where it can then be transported by the large-scale flow reaching heights of 2500 m and some tracer is advected above the marine boundary layer by coastal outflow. The overall importance of turbulent mixing and large-scale ascent in the ventilation of the boundary layer is discussed in section 8.

### 6.3. Advection, Turbulent Mixing, and Convection

[31] Consider now the role of convection. Figure 14 shows the tracer in the free troposphere integrated over height for the case in which the tracer is transported by advection, convection and turbulent mixing. These figures are dramatically different from Figures 5 and 12 showing that convection is an important process on this day. By 1300 UTC, Figure 14a, there is tracer in the free troposphere over most of the land. By 1700 UTC, Figure 14b, the amount of tracer in the free troposphere has increased as convection continues to transport tracer into the free troposphere throughout the day. Tracer that has been transported into the free troposphere is advected southeastward over France while tracer that remains within the boundary layer is advected southwestward into the north Atlantic (not shown).

[32] Figure 15 shows vertical cross sections of tracer concentration for the tracer transported by advection, mixing and convection. At 0900 UTC, Figure 15a, the tracer distribution is very similar to Figure 13a when transport is by advection and turbulent mixing only. Tracer has been mixed throughout the depth of the boundary layer over land and advection has transported tracer into the marine boundary layer over the sea. A small amount of tracer has been transported up to the free tropospheric stable layer at 3500 m. By 1300 UTC, Figure 15b, the amount of tracer that has been transported up to 3500 m has increased as convection continues to transport tracer vertically. Again, we can see a maximum in tracer concentration at the coast, but the concentration is lower than for the tracer transported by advection and turbulent mixing as convection has reduced the amount of tracer in the boundary layer. By 1700 UTC, Figure 15c, the tracer transported to 3500 m has formed a distinct layer. This separate layer is transported faster in the horizontal than the tracer that remains within the boundary layer. Thus including convection transports more tracer into the free troposphere, transports tracer higher up in the atmosphere and reduces tracer in the boundary layer so less is available for transport by coastal outflow and the sea breeze circulation. The overall importance of this shallow convection in ventilating the boundary layer is discussed in section 8.

## 7. Comparison With Observations

[33] In this section the results from the 3-D model simulation will be compared qualitatively to the CO measurements taken during the AMPEP campaign (http://badc.nerc.ac.uk/data/polluted-tropo/projects/ampep.html). CO was the chemical measured in AMPEP that is most similar to a passive tracer. It is emitted in urban areas and has a lifetime of about 2 months. We do not expect quantitative agreement between the tracer and measured CO because we have used an idealized tracer distribution. Nevertheless it is

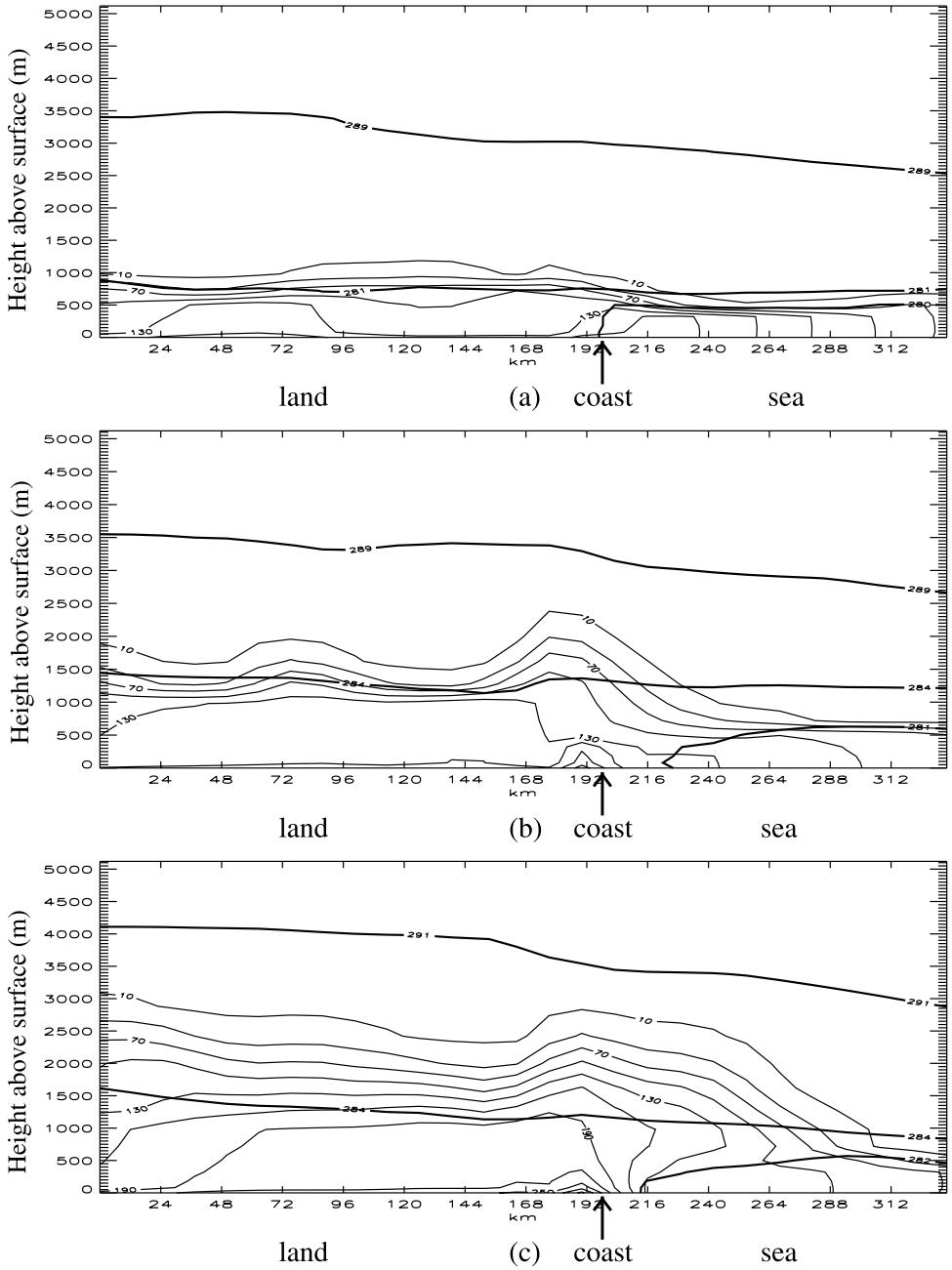


**Figure 13.** Vertical cross sections of tracer concentration, contours every $30 \times 10^{-7}$ kg/kg starting at $10 \times 10^{-7}$ kg/kg, overlaid with potential temperature contours from Figure 5, at (a) 0900 UTC, (b) 1300 UTC and (c) 1700 UTC. Tracer transported by advection and turbulent mixing.

interesting to make qualitative comparisons. Qualitative comparisons between the model tracer that is transported by advection, turbulent mixing and convection and the AMPEP CO measurements are made. Three profiles have been chosen for comparison. Profile I is over the land and it shows the depth of the boundary layer. Profile G is off the south coast of the UK and it shows high CO concentrations above the boundary layer, due to convection. Profile E is also off the south coast of the UK and it shows low CO concentrations in the boundary layer, due to the sea breeze.

[34] Figure 16 shows the model tracer profiles at different times, Figure 16a, and the AMPEP CO mixing ratio profile, Figure 16b, for vertical profile I in the middle of the UK. A second profile, profile D, has also been plotted. Profile D was taken out in the North Sea to provide a background reference CO mixing ratio for this day as the air there is unpolluted. The model tracer profile at this location shows no tracer (and is not shown here). The model tracer profile at location I at 0600 UTC shows that the tracer is trapped within the lowest 650 m of the atmosphere. By 1200 UTC the model tracer has been uniformly mixed up to 1200 m, it then decreases sharply up to 1600 m. A second peak in tracer concentration can be seen between 3000 m and 4000 m. This is the tracer that has been transported by

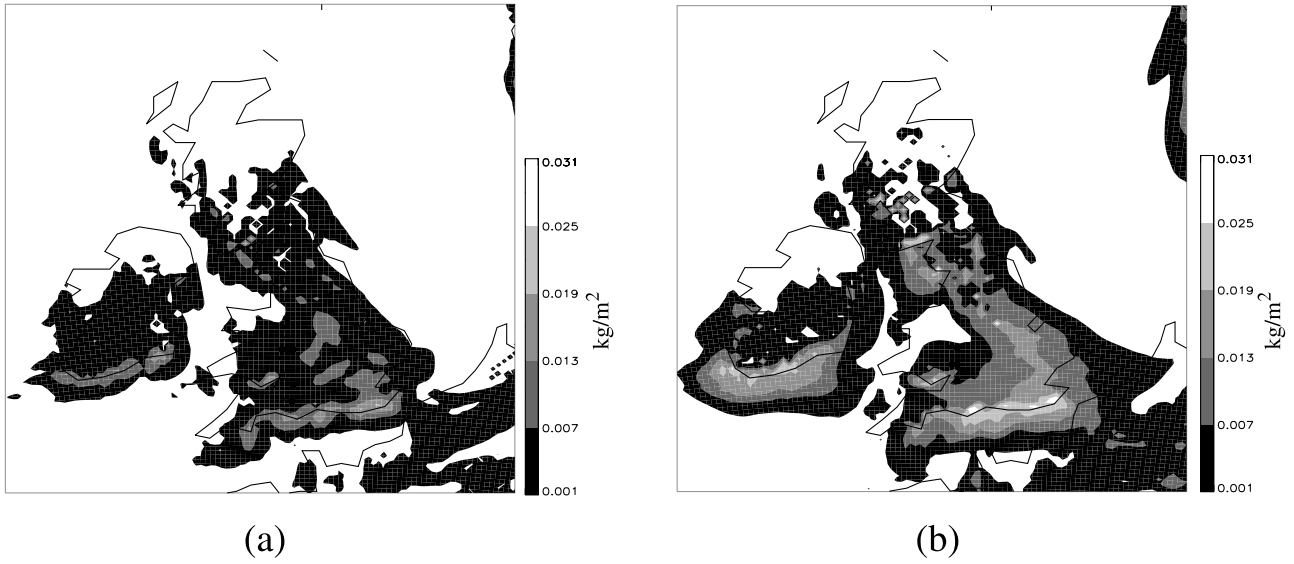


**Figure 14.** Tracer in the free troposphere integrated over height, contours every 0.006 kg/m$^2$ at (a) 1300 UTC and (b) 1700 UTC. Tracer transported by advection, turbulent mixing and convection. Note that the shading scale is the same as in Figure 12 but different to Figure 5.

convection. Comparing the model tracer profile at 1800 UTC with the AMPEP CO mixing profile I taken at 1724 UTC we see that both show a well mixed layer extending from the surface to 2000 m and then a sharp decrease to background concentrations. The aircraft levels off at 1500 m, 1100 m and 500 m to collect data which accounts for the multiple values at these levels. The feature at 500 m is probably not real. The model profile shows a second peak at 3300 m however the flight profile does not extend this far into the atmosphere. A later model profile taken at 2100 UTC shows the mixed layer height has reduced to 1000 m and the upper peak has reduced in magnitude and is located lower down.

[35] Figure 17 shows the model tracer profiles, Figure 17a, and the AMPEP CO mixing ratio profiles, Figure 17b, for profiles F and G over the sea. The model tracer profiles show that initially tracer is confined to the marine boundary layer (<500 m) at 0600 UTC and 0900 UTC. This tracer is simply being advected off the land. The concentration of tracer increases between 0600 UTC and 0900 UTC because the land-sea temperature difference increases and leads to an onshore wind acting in the opposite direction to the prevailing wind (a sea breeze front). The resulting convergence leads to an increase in the concentration of tracer until the sea breeze is strong enough to advect polluted air back toward the land. By 1500 UTC two features appear in the profile. Firstly, a peak in tracer concentration is seen between 2000 m and 3000 m. This peak is due to tracer being transported out of the boundary layer by convection over land and advected over the ocean. Secondly, the amount of tracer within the boundary layer has reduced from its 0900 UTC concentration value. This reduction in the amount of boundary layer tracer is due to the sea breeze that pushes back the tracer that has been advected over the ocean toward the land. The AMPEP flight CO mixing ratio profile G is shown in Figure 17b. Between 500 m and 1000 m CO is decreasing with height. Above 1000 m CO begins to increase with height. This profile was taken at 1530 UTC and the main features compare well qualitatively with the model tracer profile at 1500 UTC. The flight profile does not go high enough to fully capture the second peak between 2000 m and 3000 m but the increase in CO with height agrees well with the model simulation. The AMPEP flight CO mixing profile F also shows increasing CO mixing with height above 1000 m. By 2100 UTC the tracer in the boundary layer has increased again. Also seen at 2100 UTC is an increase in the concentration of tracer between 750 m and 1500 m. The tracer in this layer has been transported above the marine boundary layer by coastal outflow and is being advected over the sea. This layer of tracer is being advected at a slower speed than the convected tracer between 2000 m and 3000 m and hence appears later in the day.

[36] Figure 18a shows the model tracer profiles for vertical profile E, Figure 18a, and the AMPEP CO mixing ratio profiles for vertical profile E, Figure 18b. At 0900 UTC all of the model tracer is trapped within the marine boundary layer. At 1200 UTC the tracer concentration within the marine boundary layer has reduced and the tracer concentration at 3000 m has increased. By 1500 UTC there is further reduced tracer concentration within the marine boundary layer but a layer of polluted air has begun to emerge between 500 m and 1000 m because of coastal outflow. By 1800 UTC there is more tracer in this layer than below 500 m. This is due to the sea breeze advecting clean air back toward the land. The AMPEP flight profile E shows very low levels (almost as low as the background concentrations measured in profile D) of CO mixing ratio at 1506 UTC, well mixed below 1000 m. Hence the CO mixing ratio observed in the boundary layer appears to be less than that seen in the simulations (given that the background concentration in our simulations is zero). This may indicate that the model simulation of the sea breeze is weaker than in reality (a horizontal resolution of 12 km is

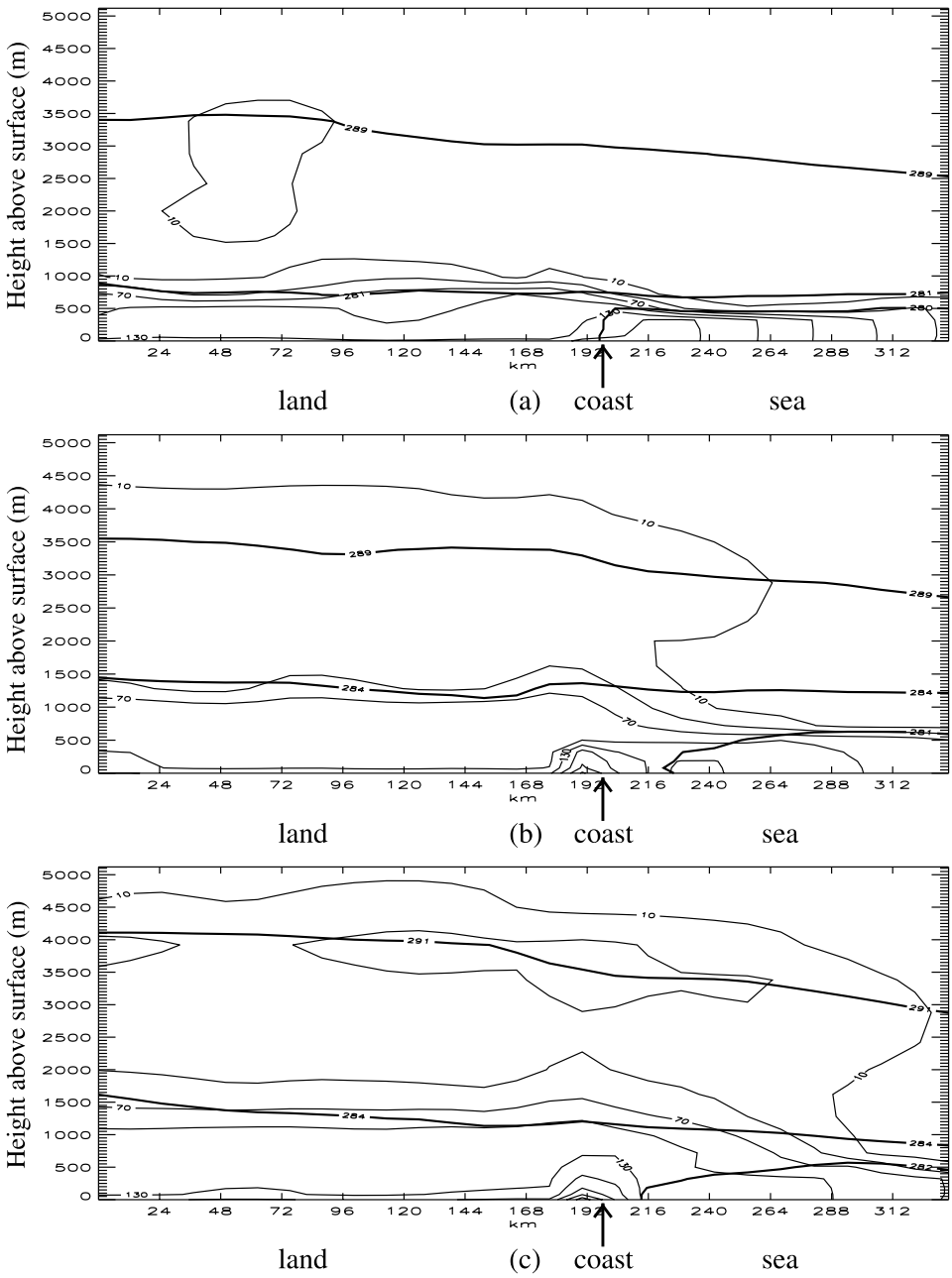


**Figure 15.** Vertical cross sections of tracer concentration, contours every $30 \times 10^{-7}$ kg/kg starting at $10 \times 10^{-7}$ kg/kg, overlaid with potential temperature contours from Figure 5, at (a) 0900 UTC, (b) 1300 UTC and (c) 1700 UTC. Tracer transported by advection, turbulent mixing and convection.

fairly coarse resolution for representing a sea breeze and it is possible that the model has underrepresented it) or may be because we have used idealized emissions in our simulations. However, given these idealized emissions, the overall agreement between the model simulated tracer distribution and the measured CO distribution is surprisingly good.

## 8. Budgets of Tracer Transport

[37] Tropospheric tracer budgets have been calculated for this case study by integrating the free tropospheric tracer mass over the region shown in Figures 5, 12 and 14. Figure 19a shows the percentage of tracer in the free troposphere for each tracer. By 0300 UTC over 40% of the tracer transported by advection and turbulent mixing is in the free troposphere. This is because at 0300 UTC the boundary layer height over land is only one or two model levels deep (i.e.,<100 m) and so only a small amount of vertical motion is needed to transport tracer out of the boundary layer. During the morning, turbulent mixing increases the depth of the boundary layer and hence the tracer is reabsorbed back into the boundary layer. This explains the peak in the percentage of the tracers in the free troposphere between 0200 UTC and 0700 UTC hours. Between 0900 UTC and 1500 UTC the percentage of tracer in the free troposphere transported by both advection and

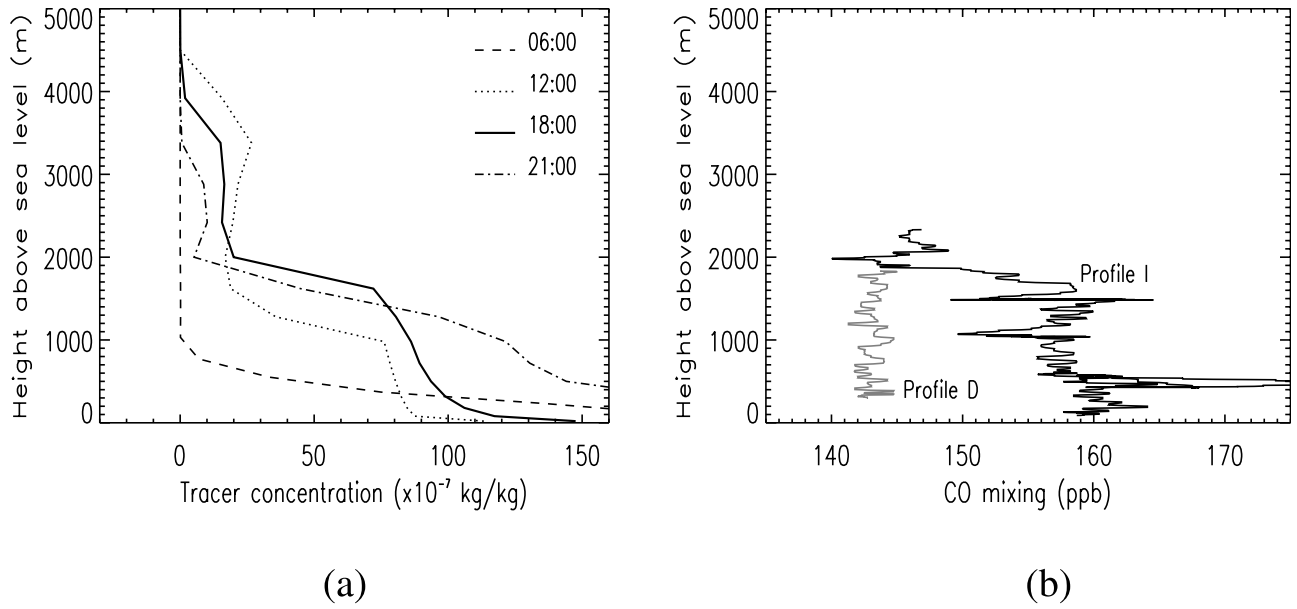


**Figure 16.** (a) Model tracer profile I at selected times and (b) AMPEP CO mixing profile D (left curve) at 1300 UTC and AMPEP CO mixing profile I (right curve) at 1724 UTC.

turbulent mixing and by advection, turbulent mixing and convection increases. However the difference between these two curves gradually increases. This is because convection is continually transporting extra tracer into the free troposphere. By 1800 UTC, when the boundary layer height collapses, 52% of the tracer transported by advection, turbulent mixing and convection and 46% of the tracer transported by advection and turbulent mixing is in the free troposphere. At 1200 UTC, when the sea breeze starts, the percentage of tracer transported by advection begins to increase from 0% to 26% by 1800 UTC. At 1800 UTC the height of the boundary layer collapses. This leads to a sharp increase in the percentage of free tropospheric tracer as tracer that was within the boundary layer now finds itself above the boundary layer top. Even during a nonfrontal day over half of the tracer emitted in the boundary layer is transported to the free troposphere. Turbulent mixing and convective processes doubled the amount of ventilation and hence need to be represented in chemical transport models.

[38] The further tracer is removed vertically from the boundary layer the further it is likely to be horizontally transported. Figure 19b shows the percentage of tracer above 2000 m for each tracer. At the beginning of the day all of the tracers remain below 2000 m. After 0900 UTC

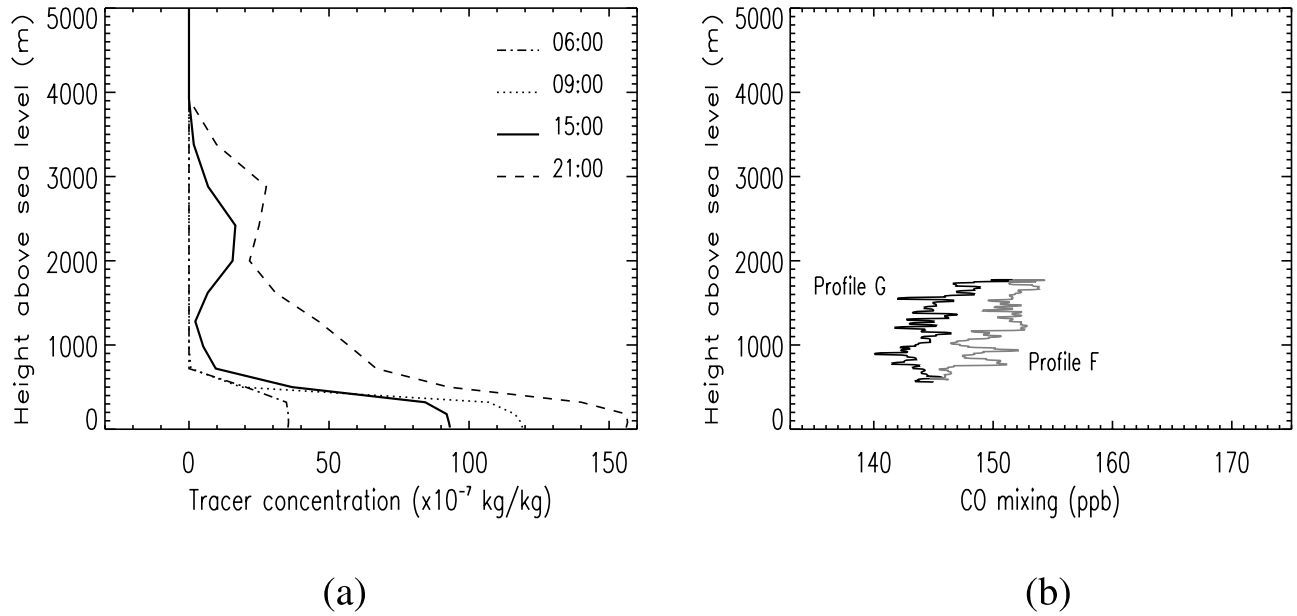


**Figure 17.** (a) Model tracer profile G at selected times and (b) AMPEP CO mixing and profile F at 1524 UTC (right curve) and profile G at 1534 UTC (left curve).

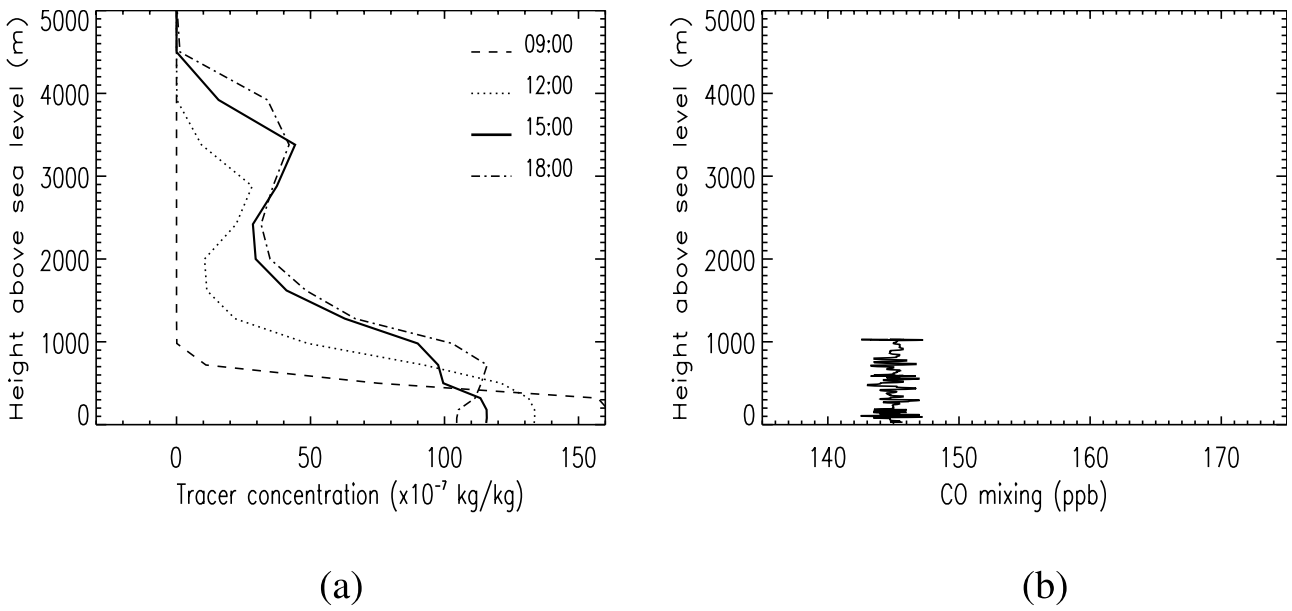


**Figure 18.** (a) Model tracer profile E at selected times and (b) AMPEP CO mixing profile E at 1506 UTC.

there is an increase in the percentage of tracer above 2000 m for the tracer that is transported by advection, turbulent mixing and convection. This is due to tracer being transported out of the boundary layer in the convective updraughts. It reaches a peak of 26% at 1700 UTC when convection dies down and then begins to decrease because tracer is being advected out of the domain. Advection and turbulent mixing transports a maximum of 10% of the tracer above 2000 m, while only 2% of the tracer transported by advection only is transported above 2000 m. Thus convection is essential to transport tracer high in the atmosphere where it is likely to become sheared from the low-level tracer.

[39] We have seen from the vertical cross sections in Figures 13 and 15 that some tracer remains just above the boundary layer top staying connected to the boundary layer tracer. This tracer has been transported above the boundary layer top by turbulent mixing followed by large-scale ascent. The amount of tracer transported will thus be sensitive to the definition of the boundary layer height. By contrast, tracer transported out of the boundary layer by convection reaches 3.5 km and so is not sensitive to the definition of the boundary layer. While the precise percentages of transport by each process will change if a slightly higher or lower boundary layer top definition is used the main conclusion, that the processes identified can all lead

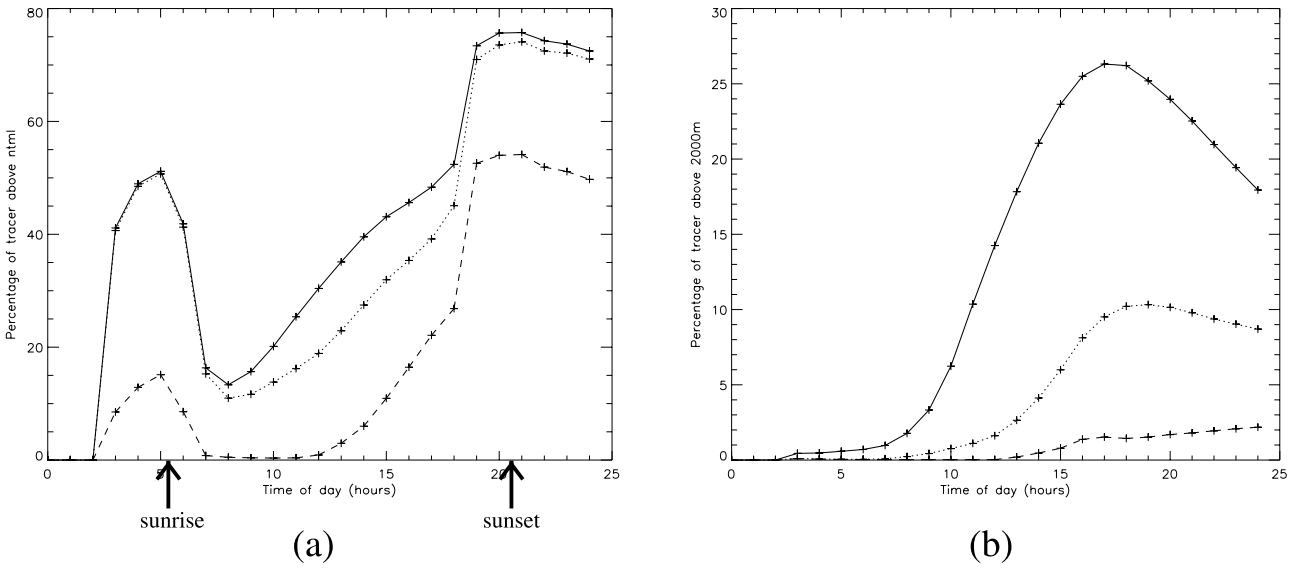


**Figure 19.** Time series of tracer integrated over the domain shown in Figure 7a. Percentage of tracer above (a) the boundary layer and (b) 2000 m. Tracer transported by advection (dashed); advection and turbulent mixing (dotted); and advection, turbulent mixing and convection (solid).

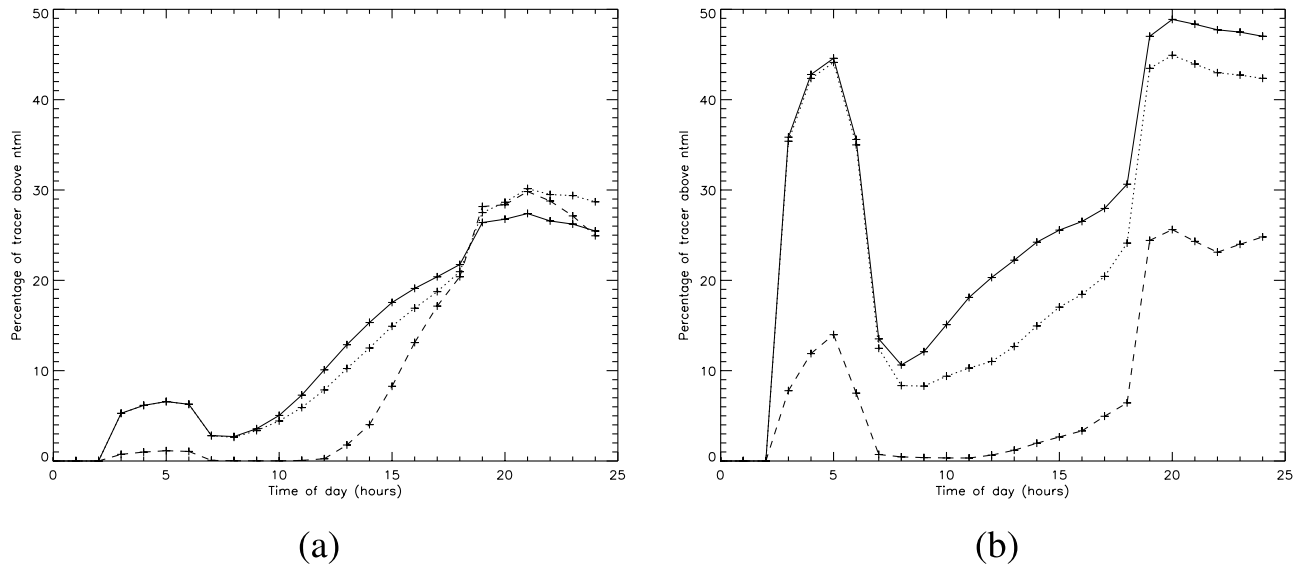


**Figure 20.** Time series of tracer integrated over the domain shown in Figure 7a. Percentage of tracer ventilated (a) within and (b) without the south coast domains shown in Figure 5b. Tracer transported by advection (dashed); advection and turbulent mixing (dotted); and advection, turbulent mixing and convection (solid).

to transport of pollutants and that this transport can be significant, will be unaffected.

[40] Figures 20 and 20b show the percentage of tracer transported out of the boundary layer in the vicinity of the south coasts of Ireland and England and in the remainder of the domain respectively (see Figure 5b for domains). These figures quantify of the importance of different processes in ventilating the boundary layer. Coastal outflow and the sea breeze circulation are the dominant mechanisms acting to ventilate pollution from the boundary layer along the south coasts of England and Ireland. Thus Figure 20a shows that these processes are responsible for ventilating 21% of the tracer emitted in the domain compared to 52% by all ventilation processes (these percentages are taken at 1800 UTC, just prior to the increase in tropospheric tracer due to the nocturnal collapse of the land boundary layer). Ventilation by large-scale ascent and convection are the dominant processes elsewhere in the domain. Thus Figure 20b shows that large-scale ascent is responsible for ventilating 24% of the pollution and including convection increases this to 30%. Note that these ventilation processes are not additive. Including convection, for example, will mean there is less tracer in the boundary layer to be transported by turbulent mixing, large-scale ascent, the sea breeze circulation and coastal outflow.

## 9. Conclusions

[41] The UK Met Office Unified Model has been used to simulate the transport processes that occurred during a nonfrontal day on the 9 May 2005. This was a typical UK summer day with little wind and scattered shallow cumulus convection. Model simulated vertical tracer distribution qualitatively compared well with AMPEP flight measurements in most cases. Therefore we can conclude that numerical weather prediction model output is a useful tool in these situations and can be used to complement observational results in studying transport processes.

[42] The ventilation processes observed on the 9 May 2005 include coastal outflow, ventilation by the sea breeze circulation, ventilation by turbulent mixing and large-scale ascent, and ventilation by convection. The ventilation through a diurnal cycle is shown schematically in Figure 21:

[43] 1. In the early morning before sunrise the boundary layer over the land is shallower than the boundary layer over the sea. Both are capped by low-level stable layers. An additional stable layer exists in the free troposphere on the day of the case study.

[44] 2. During the morning surface heating leads to turbulent mixing over land. Entrainment of air from above the boundary layer top increases the depth of the boundary layer over land. The boundary layer is now deeper over land than over the sea. Two low-level stable layers are observed over the sea. One is the internal marine boundary layer and the other is the stable layer capping the land boundary layer which is advected over the sea.

[45] 3. During the afternoon further surface heating leads to convection and cumulus clouds over land and a sea breeze at the coast. Convection penetrates the boundary layer top but is capped by a stable layer in the free troposphere on this day. Convergence between the sea breeze and the prevailing wind leads to vertical advection of pollution near the coast. Horizontal advection of pollution across the coast transports pollution above the marine boundary layer (coastal outflow). Pollution is trapped between the marine boundary layer and the advected land boundary layer.

[46] 4. During the evening after sunset the boundary layer over the land collapses. The boundary layer over the sea is now deeper than over the land. Two residual layers of pollution, one due ventilation by convection and one due

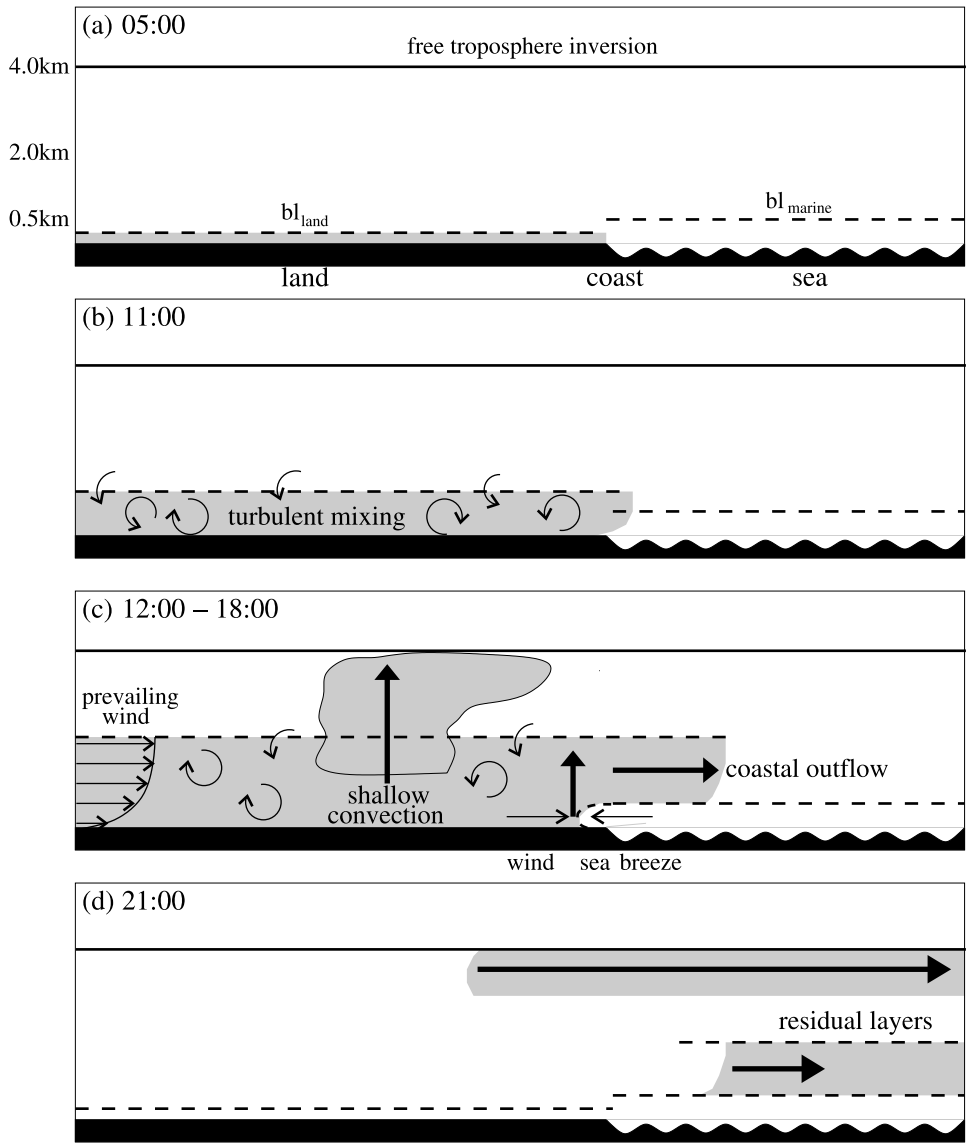


**Figure 21.** Schematic of ventilation processes during this case study. $bl_{land}$ and $bl_{marine}$ are stable layers at the top of the land and sea boundary layers, respectively. (a) Before sunrise $bl_{marine}$ is deeper than $bl_{land}$. (b) After sunrise turbulent mixing increases the depth of $bl_{land}$ while $bl_{marine}$ remains fairly constant. (c) In the afternoon the boundary layer is ventilated by shallow convection, coastal outflow and the sea breeze circulation. (d) After sunset residual layers of pollution are advected downwind.

to coastal outflow, are advected downwind at different speeds and in different directions.

[47] During this particular nonfrontal day advection, turbulent mixing and convection processes together ventilated 52% of the emitted tracer into the free troposphere by 1800 UTC of which 26% was above 2 km. Note that while the precise percentages of tracer located in the free troposphere will depend on the definition of boundary layer height used, all the processes described here cause boundary layer ventilation. Turbulent mixing and convection processes double the amount of pollution ventilated from the boundary layer. This case reveals the transport processes that can occur in the absence of fronts and demonstrates that they can lead to significant ventilation of the boundary layer. This suggests that significant ventilation can also occur on high-pressure days, particularly if they are associated with shallow convection and/or a sea breeze circulation. However, the relative magnitudes of transports by these processes will vary on a case-by-case basis.

[48] **Acknowledgments.** We would like to thank the Met Office for use of their Unified Model. We are also grateful to Chang-Gui Wang for the use of her data visualization program provided through the Universities Weather Research Network. We also thank Debbie Polson for help with the

AMPEP data and all of the AMPEP team for taking the aircraft measurements. Helen Dacre was supported by a NERC grant.

## References


Agustí-Panareda, A., S. L. Gray, and J. Methven (2005), Numerical modeling study of boundary-layer ventilation by a cold front over Europe, *J. Geophys. Res.*, *110*, D18304, doi:10.1029/2004JD005555.

Angevine, W. M., M. Tjernstrom, and M. Zagar (2006), Modeling of the coastal boundary layer and pollutant transport in New England, *J. Appl. Meteorol. Climatol.*, *138*(45), 137–154.

Baltensperger, U., H. W. Gaggeler, D. T. Jost, M. Lugauer, M. Schwikowski, E. Weingartner, and P. Seibert (1997), Aerosol climatology at the high-alpine site Jungfraujoch, Switzerland, *J. Geophys. Res.*, *102*, 19,707–19,715.

Chatfield, R. B., and P. J. Crutzen (1984), Sulfur dioxide in remote oceanic air: Cloud transport of reactive precursors, *J. Geophys. Res.*, *89*, 7111–7132.

Cullen, M. (1993), The unified forecast/climate model, *Meteorol. Mag.*, *122*, 81–94.

Dickerson, R. R., et al. (1987), Thunderstorms: An important mechanism in the tranport of air pollutants, *Science*, *235*, 460–465.

Donnell, E. A., D. J. Fish, and E. M. Dicks (2001), Mechanisms for pollutant transport between the boundary layer and the free troposphere, *J. Geophys. Res.*, *106*(D8), 7847–7856.

Edy, J., S. Cautenet, and P. Bremaud (1996), Modeling ozone and carbon monoxide redistribution by shallow convection over the Amazonian rain forest, *J. Geophys. Res.*, *101*(D22), 28,671–28,681.

Esler, J. G., P. H. Haynes, K. S. Law, H. Barjat, K. Dewey, J. Kent, and S. Schmitgen (2003), Transport and mixing between airmasses in cold frontal regions during Dynamics and Chemistry of Frontal Zones (DCFZ), *J. Geophys. Res.*, *108*(D4), 4142, doi:10.1029/2001JD001494.

Flatøy, F., and Ø. Hov (1995), Three-dimensional model studies of exchange processes of ozone in the troposphere over Europe, *J. Geophys. Res.*, *100*(D6), 11,465–11,481.

Gimson, N. R. (1997), Pollution transport by convective clouds in a mesoscale model, *Q. J. R. Meteorol. Soc.*, *123*, 1805–1828.

Gray, S. L. (2003), A case study of stratosphere to troposphere transport: The role of convective transport and the sensitivity to model resolution, *J. Geophys. Res.*, *108*(D18), 4590, doi:10.1029/2002JD003317.

Gregory, D., and P. R. Rowntree (1990), A mass flux convection scheme with representation of cloud ensemble characteristics and stability dependent closure, *Mon. Weather Rev.*, *118*, 1483–1506.

Hauf, T., P. Schulte, R. Alheit, and H. Schlager (1995), Rapid vertical tracer gas transport by an isolated midlatitude thunderstorm, *J. Geophys. Res.*, *100*(D11), 22,957–22,970.

Hobbs, P. V. (2000), *Introduction to Atmospheric Chemistry*, Cambridge Univ. Press, Cambridge, U. K.

Kossmann, M., U. Corsmeier, S. De Wekker, F. Fiedler, R. Vögtlin, N. Kalthoff, H. Güstin, and B. Neininger (1999), Observations of handover processes between the atmospheric boundary layer and the free troposphere overm ountainous terrain, *Contrib. Atmos. Phys.*, *72*, 329–350.

Kowol-Santen, J., M. Beekman, S. Schmitgen, and K. Dewey (2001), Tracer analysis of transport from the boundary layer to the free troposphere, *Geophys. Res. Let.*, *28*, 2907–2910.

Leon, J.-F., et al. (2001), Large-scale advection of continental aerosols during INDOEX, *J. Geophys. Res.*, *106*(D22), 28,427–28,439.

Lock, A. P., A. R. Brown, M. R. Bush, G. M. Martin, and R. N. B. Smith (2000), A new boundary layer mixing scheme. Part 1. Scheme description and single-column model tests, *Mon. Weather Rev.*, *128*, 187–199.

Lu, R., and R. Turco (1994), Air pollutant transport in a coastal environment. Part I: Two-dimensional simulations of sea-breeze and mountain effects, *J. Atmos. Sci.*, *51*, 2285–2308.

Lu, R., C. Lin, R. Turco, and A. Arakawa (2000), Cumulus transport of chemical tracers: 1. Cloud-resolving model simulations, *J. Geophys. Res.*, *105*(D8), 10,001–10,021.

Schultz, P., and T. T. Warner (1982), Characteristics of summertime circulations and pollutant ventilation in the Los Angeles basin, *J. Appl. Meteorol.*, *21*, 672–682.

Seibert, P., H. Kromp-Kolb, A. Kasper, M. Kalina, H. Puxbaum, D. T. Jost, M. Schwikowski, and U. Baltensperger (1998), Transport of polluted boundary layer air from the Po Valley to high-alpine sites, *Atmos. Environ.*, *32*, 3953–3965.

Smith, F. B. (1975), Airborne transport of sulphur dioxide from the United Kingdom, *Atmos. Environ.*, *9*, 643–659.

Thompson, A. M., K. E. Pickering, R. R. Dickerson, W. G. Ellis Jr., D. J. Jacob, J. R. Scala, W.-K. Tao, D. P. McNamara, and J. Simpson (1994), Convective transport over the central United States and its rode in regional CO and ozone budgets, *J. Geophys. Res.*, *99*(D9), 18,703–18,711.

Verma, S., O. Boucher, C. Vendataraman, M. S. Reddy, D. Muller, P. Chazette, and B. Crouzille (2006), Aerosol lofting from sea breeze during the Indian Ocean experiment, *J. Geophys. Res.*, *111*, D07208, doi:10.1029/2005JD005953.

Wakimoto, R. M., and J. L. McElroy (1986), Lidar observation of elevated pollution layers over Los Angeles, *J. Clim. Appl. Meteorol.*, *25*, 1583–1599.

Wang, C., and R. G. Prinn (2000), On the roles of deep convective clouds in tropospheric chemistry, *J. Geophys. Res.*, *105*(D17), 22,269–22,287.

Wilson, D. R., and S. P. Ballard (1999), A microphysically based precipitation scheme for the UK Meteorological Office unified model, *Q. J. R. Meteorol. Soc.*, *125*, 1607–1636.


S. E. Belcher, H. F. Dacre, and S. L. Gray, Department of Meteorology, University of Reading, Earley Gate, PO Box 243, Reading RG6 6BB, UK. (h.f.dacre@reading.ac.uk)